2018 7th IEEE International Conference on Biomedical
Robotics and Biomechatronics (Biorob)
Enschede, The Netherlands, August 26-29, 2018

Design and Preliminary Evaluation of a 3-DOF Powered Prosthetic Wrist Device

Neil M. Bajaj, *Student Member*, IEEE, and Aaron M. Dollar, *Senior Member*, IEEE

***Abstract*— Though the human wrist greatly benefits manipulation by orienting the hand, recreating its functionality in anthropomorphic proportions proves to be difficult. As a result, upper limb amputees who desire wrist functionality must often use often passive single degree of freedom devices to attempt to recover some of this missing ability. In this work, the authors present the preliminary design and kinematic testing of a 3 DOF actuated wrist prosthesis. The device is capable of 90 degrees of circumduction (combined flexion and abduction), and continuous rotation in pronation. The circumducting portion of the wrist is composed of a parallel mechanism, while the pronation drive is a belt-driven serial mechanism. The circumducting DOFs are actuated via nonbackdrivable linear DC motors, and the gear ratio and friction of the pronation mechanism make it nonbackdrivable under reasonable loads as well. The architecture of this wrist was chosen such that when the device is integrated into a transradial socket, the motors could be placed on the socket periphery, allowing amputees with long residual limbs to use the wrist without significantly offsetting the terminal device. Benchtop evaluation of the wrist device is performed to evaluate the speed of the wrist in actuation from the neutral position to a variety of flexion and abduction positions, as well as to evaluate its pronation speed. We find the wrist performs rather near to the ideally expected speed values.**

I. Introduction

The function of the human wrist is to allow the hand to achieve a large number of 3 degree of freedom (DoF) orientations without significantly reorienting the more proximal portions of the arm. Though many 3DoF spherical orientation mechanisms exist [1]–[3], achieving the same compactness and weight of the human forearm and wrist while maintaining the same level of functionality is prohibitively difficult. Losing wrist mobility, either through immobilization or amputation, can lead to significant compensatory movements [4], [5]. These movements can lead to undue strain on proximal unaffected joints which do not undergo such large motions in unaffected individuals.

Within upper limb prosthetics, a large portion of development focuses on creating terminal devices with greater mobility, speed, or to seem more anthropomorphic. In contrast, development of wrist prostheses is rather slow, with most commercially available devices limited to single DoF passive rotators [6]. Currently, there are no multi-DoF standalone powered wrist prostheses that are commercially available. Few are found in larger arm prostheses, but a variety of factors tend to make them difficult to adapt for use for individuals with transradial or transhumeral amputation. However, passive prostheses with active elements that alter the stiffness have been developed recently [7], [8] and show potential benefits, especially with regards to size, weight, and manipulation capacity.

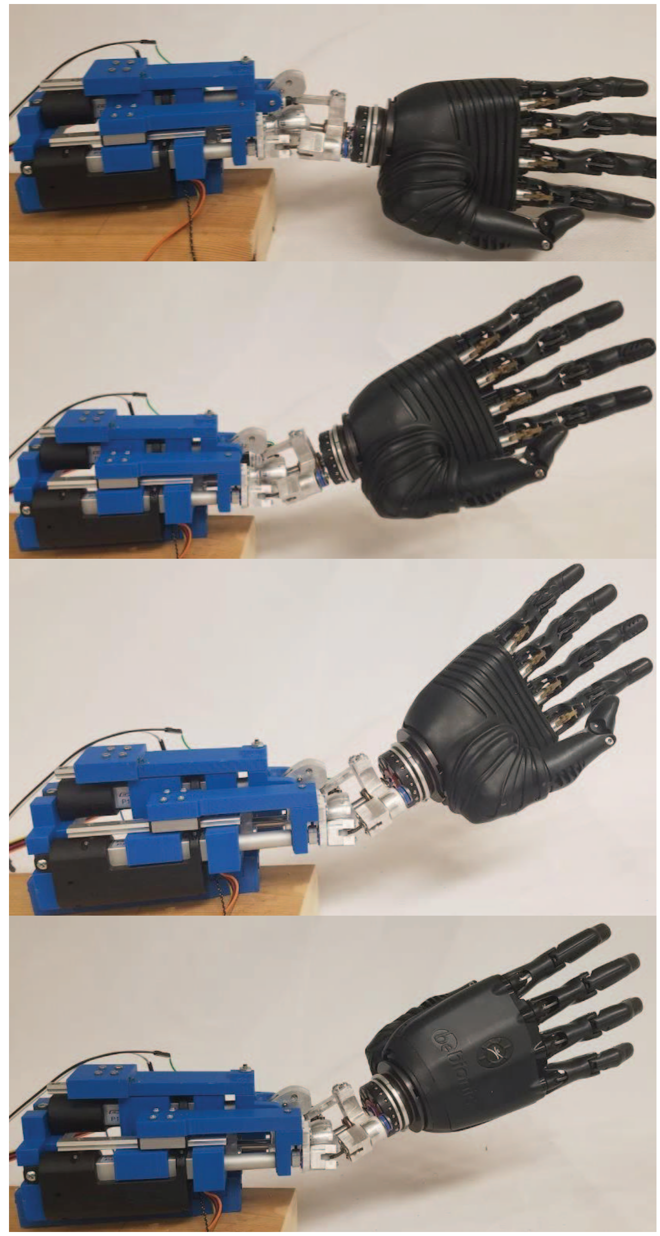

Fig. 1. The prototype wrist moving actuating through its three DoF with the Bebionic v2 hand.

* This work was supported by the US Army Medical Research and Materiel Command, under contract W81XWH-15-C-0125. The authors are with the Department of Mechanical Engineering and Materials Science, University, New Haven, CT 06511 (email: neil.bajaj@yale.edu; aaron.dollar@yale.edu).

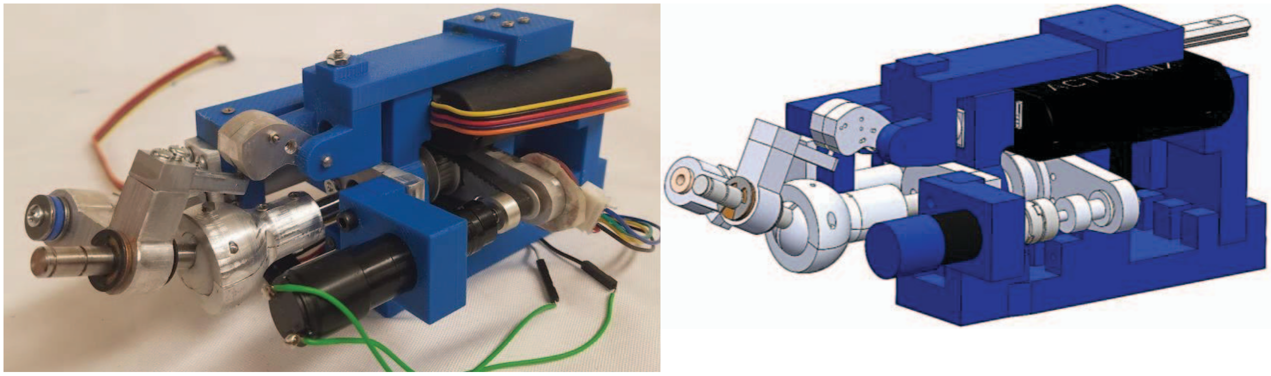

Fig. 2. Prosthetic wrist prototype (left) and idealized CAD model (right).

Recent investigations [9] have found that wrist dexterity may contribute as much to human mobility as much as a fully dexterous, highly mobile hand. While both hand and wrist prostheses cannot yet emulate the ability of their unaffected human counterparts, a 3DOF wrist may be easier to design, control, and fabricate than a fully actuated anthropomorphic hand.

In this paper, we introduce a novel 3DoF prototype of a powered wrist (Fig. 1, Fig. 2) prosthesis suitable for use with transradial and more proximal amputees. By utilizing a hybrid mechanism architecture, we combine the benefits of serial mechanisms (such as simplicity and large workspace) with the advantages of parallel mechanisms (higher stiffness to size and variety of actuator placement). The entire wrist is sized to mimic the size of the 50th percentile human male forearm. The choice of actuators and drive train elements make the wrist nonbackdrivable, thereby consuming no power when the device is off. Furthermore, the actuator selection also allows the size of the wrist to be increased or decreased, and allows the wrist to be integrated into a transradial socket.

In the following section, we detail the hardware design of the wrist device, describing the portions of the wrist responsible for each output DoF. Subsequently, we discuss the preliminary testing plan to evaluate the speed. We conclude with a discussion of future development directions for the wrist and subsequent evaluations of the device.

II. Mechanical Design

A. Design Overview

The wrist is composed of three actuation modules: the pronation module, flexion module, and the abduction module. Each module is named by the output DOF it actuates. The pronation mechanism is a simple serial chain whereas the flexion and abduction mechanisms are both part of a parallel mechanism which serves to point the output shaft of the wrist. Kinematic analysis of the wrist architecture and an optimization over the geometric parameters was previously presented in [10]. This particular wrist implementation differs from the design yielded form the optimization by introducing constraints on the overall size and enforcing the actuators remain parallel to the long axis of the wrist.

This design can achieve circumduction with an included conic angle of 90º, and infinite distal pronation and supination. Note we choose to call this DoF distal pronation as it occurs distally to flexion and abduction, which is the reverse of the human wrist but leads to a simpler design.

The wrist length, measured from the most proximal base point to the end of the distal platform (which corresponds to how low a terminal device could seat onto the output shaft) is 18cm. The circumscribing circle of the wrist has a radius of 4.3cm. These dimensions correspond to that of a 50th percentile male [11] (forearm length 25.7cm, forearm circumference 8.6cm). The total device has a mass of 578g, with 220g belonging solely to the actuators.

B. Pronation Module

Kinematically, the pronation module (Fig. 3) is composed of a Revolute – Universal serial chain and is actuated by the revolute joint. This type of architecture is commonly used to allow for two misaligned shafts to rotate together. With this wrist, misalignment purposefully occurs due to flexion and abduction. While the input shaft stays fixed in space, the output shaft will point in the direction dictated by the flexion and abduction modules. Moreover, this architecture yields an unlimited range of motion.

The proximal input shaft is rigidly fixed to the proximal portion of the universal joint, thus rotating this shaft causes distal pronation to occur. An 18mm toothed pulley (28 teeth) is rigidly fixed to the proximal input shaft via pair of set screws. This 28-tooth pulley is driven by a smaller 10 tooth pulley on a parallel shaft. The smaller pulley is in turn driven by a geared DC motor (Faulhaber 1717012SR, 15A 249:1 gearhead). The motor and gearhead combination have a nominal no-load speed of 54rpm and a stall torque of 1.37Nm. The high gear ratio also makes the mechanism nonbackdrivable under loads slightly greater than what the pronation module itself may produce. In tandem with the pulley drive, this yields a theoretical no-load speed of 19.2rpm (115°/s) and 3.8Nm of stall torque on the input shaft. Conservatively estimating a 50% loss in total torque, this still yields 1.9Nm of torque, around 20% of maximal human effort, which is enough to turn a doorknob [12].

A belt drive was chosen because it allows for freedom in positioning the pronation motor. Adaptations and customizations or amputees with different residual limb geometry can be made in this wrist simply by repositioning the actuators and using a different belt, or via use of idler pulleys.

The proximal input shaft is supported by a pair of flanged bronze Oilite bushings to support radial and axial loads. Both of the bushings are fixed within the wrist body and do not move. The front and back faces of the larger pulley each press

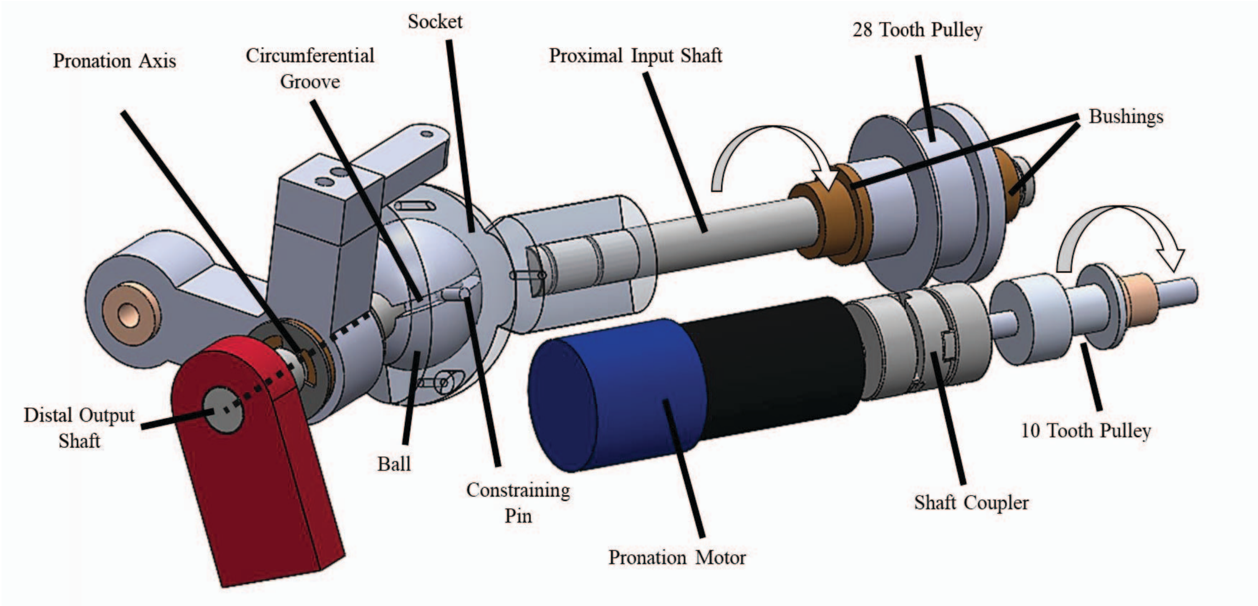

Fig. 3. Components of the pronation module, with other modules and support suppressed. The pulley belt has also been suppressed for clarity.

into a flange of one of the bushings. As the pulley is fixed on the shaft, this supports the axial loads on the shaft as well.

The motor position can be resolved through an encoder on the motor's output shaft, after the gearbox. While placing the encoder before the gearbox would allow for higher resolution, backlash within the gear system would need to be compensated for and a much faster quadrature encoder counter would be needed. Moreover, 50 pulses per revolution on the smaller pulley's shaft corresponds to 140 pulses per revolution on the larger pulley's shaft (the proximal input shaft), resulting in a resolution of 2.6º in pronation. Lockable passive pronating prosthetic wrists may be fixed in 20 discrete positions, resulting in 18° between positions. Moreover, it is unlikely that a user would require more accurate positioning in pronation during ADLs.

The proximal input shaft drives the central universal joint of the wrist. Instead of using a typical two yoke and central cross universal joint, a constrained spherical joint is used. This has a number of advantages, including a simpler workspace as interference with the yokes is eliminated (examined in [13]), and more contact / bearing area to supports loads placed on the wrist. The 1.91cm (0.75in) diameter acetal sphere is captured within the aluminum housing, which has an identically sized cavity machined out of it. The socket has a large portion machined out of the distal face which sets the range of motion for the other two DoFs.

To turn the ball and socket spherical joint into a universal joint, the ball has a circumferential groove 0.32cm (1/8th in) wide machined into the surface. This groove is locked in place via a 0.32cm (1/8th in) pin which tangentially contacts the walls of the groove. This pin is press fit into the socket and is fixed within the socket. This constrains rotational motion about the axis normal to be about the pin's symmetry axis and the groove's symmetry axis (2 DOF rotational motion). Only by rotating the entire socket can rotation about this constrained axis occur. As the socket is rigidly coupled to the proximal input shaft by set screws, the rotary motor and pulley drive spin this constrained axis. Similar constrained pin designs are used in the OttoBock Myolino [14].

As is apparent in Fig. 3, this constrained pronation axis is coincident with the distal output shaft. Due to the misalignment between the constrained axis and the input shaft, they will generally rotate at differing rates, through the relationship is cyclic, predictable, and well defined, so knowing the rotation of the proximal shaft and the actual direction of the constrained axis / distal output shaft fully determines the output shaft rotation angle.

The distal output shaft, a 0.64cm (0.25in) steel shaft, is press fit into the central acetal sphere, and the further retained by a set screw. A terminal device would be rigidly coupled to the distal output shaft when the prosthetic device is being utilized.

The other two modules constrain the axis in which the distal output shaft points. These other two DoFs are actuated by the surrounding parallel mechanism, which will be discussed in more detail in subsequent sections. The parallel mechanism serves to orient the distal platform, through which the distal output shaft passes. The shaft is supported in the platform by another pair of flanged Oilite bushings and circlip retaining rings. These prevent the platform from translating along the shaft and allow the shaft to rotate within the platform.

C. Flexion Module (Parallel Mechanism)

The flexion module (Fig. 4) is kinematically composed of a Prismatic-Revolute-Universal-Revolute serial chain. It is in parallel with the abduction module and thus forms half of the parallel mechanism. In both of these modules, the prismatic joint is actuated. The flexion axis is a fixed axis which is perpendicular to the proximal input shaft and perpendicular to the vertical plane. It does not change its position as the wrist actuates, and the flexion angle is completely determined by the flexion module.

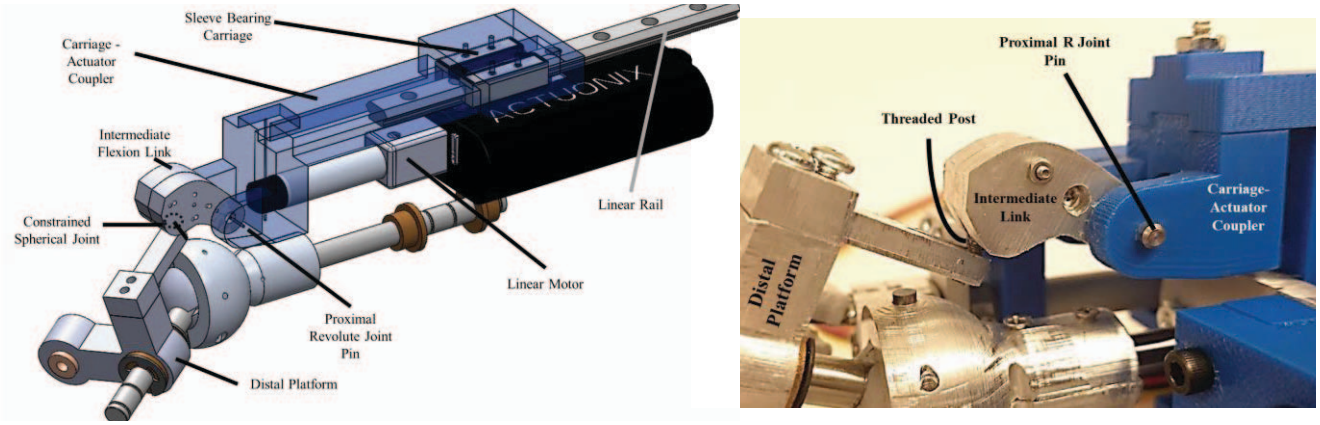

Fig. 4. Components of the flexion module. (Left) CAD representation of the flexion module, unrelated components suppressed. (Right) Closeup of the intermediate flexion link showing the threaded post.

The prismatic joints are actuated via linear motors (*Actuonix P16-50-64-12-P*). These motors have a stroke of 50mm, a stall force of 90N, and a max speed of 2.5cm/s. As the maximal stroke is required to actuate the flexion mechanism over its 90° range of motion, this flexion module could theoretically travel from maximum flexion to maximum extension in approximately two seconds. Moreover, they are nonbackdrivable, so the wrist locks in its flexion and abduction position when the actuators are turned off. The actuator line of action is parallel to the proximal input shaft and thus the intended forearm axis.

The actuators have internal linear potentiometers which can be used to determine their positions and allow for closed loop control over the actuators. As their speeds are quite low and they are nonbackdrivable, there is virtually no positional overshoot, thus a bang-bang control policy [15] is used to control their positions. The kinematics described in [10] can be used to determine the mapping between actuator position and flexion angle.

The actuators themselves cannot tolerate high side loads, so linear rails with carriage supports are used to provide resistance to side forces. The carriage slides along an extruded aluminum rail, which is screwed into auxiliary pieces attached to the actuator body. The carriage itself is screwed into a 3D printed piece carriage-actuator coupler which connects to the actuator tip. The other end of the actuator tip connects serves as the axis for the proximal revolute joint. The joint itself is composed of a 0.32cm (0.125 in) pin which is within the carriage-actuator coupler.

The carriage-actuator coupler allows the actuator itself to be moved into a convenient location while preserving its line of action. The actuator could be moved parallel to its line of action, and as long as the location of the proximal revolute joint position did not change, the kinematics would not be altered. Internal forces can arise due to this repositioning, but those forces are still borne by the carriage on the linear rail rather than the actuator's internal components. This can be leveraged when integrating this wrist design within a prosthetic socket, as the actuators may be placed distal to the residual limb for a transradial amputee with proximal amputation, or around the residual limb itself for amputees with long residual limbs.

The proximal revolute joint also serves as the rotational axis of the intermediate flexion link. The intermediate link couples motion of the linear actuator to the distal platform. On one end is the proximal revolute joint, whereas on the other is the universal joint. This universal joint is also composed of a constrained spherical joint. A 0.64cm (0.25") diameter acetal sphere sits within a spherical cavity in the intermediate link and is attached to a threaded post that passes through its center. The cutout this post pass through is a slot with the same width as the post diameter. As a result, the post cannot move laterally. It may only rotate about its own axis and about an axis parallel to the proximal revolute joint. The large supporting surface area makes this universal joint quite stiff compared to traditional universal joints of the same configuration and total overall size.

The axis of this post defines the abduction axis (Fig. 5), which is not fixed, as the post changes its position with flexion.

The aforementioned threaded post screws into the distal platform and is bonded to it so that it may not rotate relative to the threaded hole. Rotation about the post axis instead occurs in the intermediate link between the spherical cavity and the acetal sphere.

Actuating the linear motor forwards causes wrist flexion to occur, pointing the output shaft downwards. The intermediate link pivots about the proximal revolute joint, and the angle between the intermediate link (from one joint center to the other) and the distal platform changes as well. Finally, the output shaft slightly rotates during flexion in the distal revolute joint, though only by a few degrees at most.

Over its range of motion, the flexion mechanism ideally generates 2.02Nm of torque about the flexion axis, with a minimum of 0.9Nm at full extension and a maximum of 3.2Nm at full flexion. Elasticity, mechanical slop, and misalignment all serve to decrease the maximal torque production, though using the previously conservative estimate of 50% torque loss still results in 10% of average unaffected human wrist flexion torque [16].

D. *Abduction Module (Parallel Mechanism)*

The other half of the parallel mechanism is the abduction module (Fig. 5). It is kinematically composed of a Prismatic-Spherical-Spherical-Revolute chain, with the prismatic joint actuated. Many of the concepts and design features are the

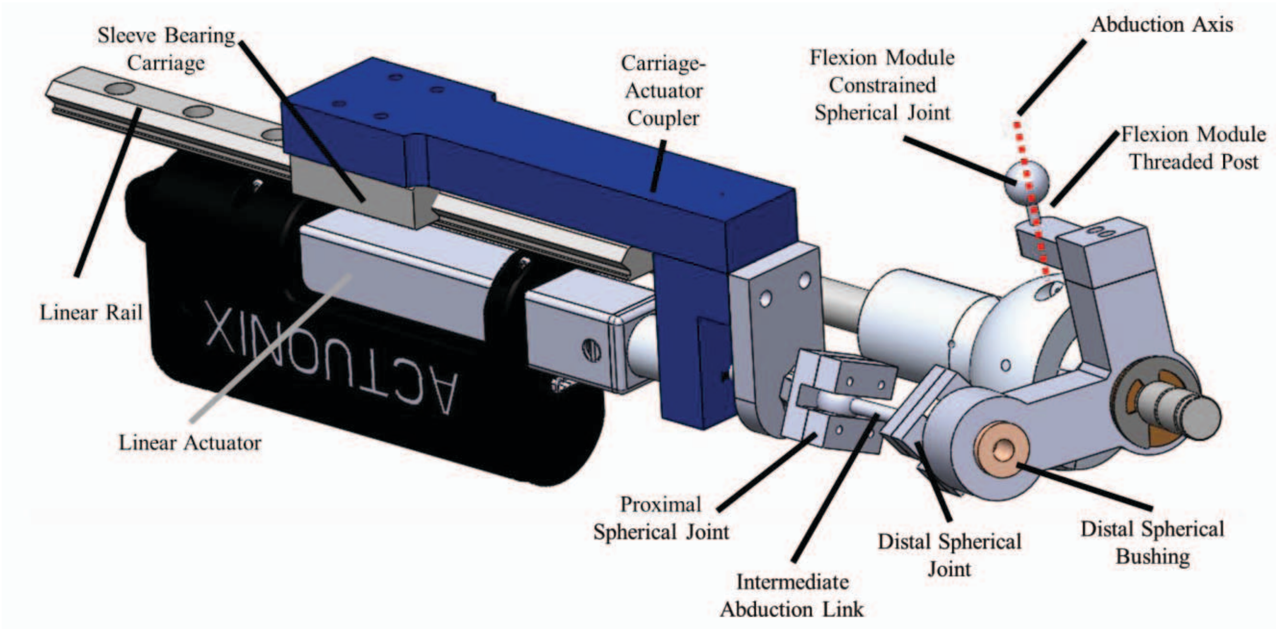

Fig. 5. Abduction mechanism key components. Note the slot in the proximal spherical joint through which the intermediate link passes. When the intermediate link contacts the slot walls, the entire spherical joint spins to allow the intermediate link to keep moving. The abduction axis is also shown

same as those in the flexion module. Namely, the usage of a linear rail, sleeve bearing carriage, carriage-actuator coupler, and control policy are identical. Moreover, the final revolute joint in each leg is the same, and corresponds to the distal output shaft which spins freely within the distal platform. A key kinematic difference is that abduction axis is not fixed. As it is coincident with the threaded post, its position is fully determined by the flexion module. Actuating the abduction motor results in abduction instantaneously about the threaded post's axis.

The intermediate abduction link lies between the two spherical joints in this leg. The link itself is simply another threaded rod, with two identical 0.64cm (0.25in) acetal spheres threaded onto either end. Each of these spheres lay captured within identical spherical joint housings.

These spherical joint housings are similar to the spherical joint cavity machined in the intermediate flexion link. They both have long slots only slightly wider than the diameter of the threaded rod. However, the entire spherical joint housing may rotate relative to the component it attaches to as well. The proximal spherical joint housing rotates about the prismatic joint line of action, and the distal joint housing rotates about the axis of the bushing in the distal platform (Fig. 5).

When the intermediate link makes contact with the walls of the slot, this causes a torque about the spherical joint housing's attachment axis. The entire housing will then turn if the force the intermediate link applies to the slow wall can overcome the small amount of turning friction. These spherical joints thus have high ranges of motion - greater than 180º if necessary. Other work has been done to increase the range of motion of universal and spherical joints [17] using redundant joints, though this solution more easily met the size constraints and load requirements.

The overall ideal actuation time of the abduction module is the same as the flexion module, through the torque performance is different. The average torque over its range of motion is 1.6Nm, with a maximum of 2.6Nm at maximal abduction (actuator retracted completely) and a minimum of 0.8Nm at full extension. If kinematic constraints were relaxed and the linear actuators were allowed to be cast inwards at angles relative to the proximal input shaft, then the torque performance of this module could be significantly improved.

III. Benchtop Testing Protocol

A. *Parallel Mechanism Evaluation*

To evaluate the hardware implementation of the prosthetic wrist prototype, benchtop testing was performed. In this testing, we evaluated the wrist from a kinematic viewpoint by examining the time it takes to actuate from the neutral position to a variety of flexed and abducted position. Specifically, we operated the wrist in bang-bang position control and had it actuate to one of 40 discrete points in the circumduction workspace. The time it took to reach that point from the neutral position as well as the time it took to return was recorded. Each test was repeated 10 times and the average time of actuation to each point and the time it took to return from that point was recorded. The actuators were controlled using a microcontroller (*Arduino Micro ATmega32U4*) and H-Bridges (*Texas Instruments SN754410*) connected to a DC power supply at 12V with a current limit of 5A. The microcontroller executed the position control loop at 200 Hz and handled timing measurement as well.

These measurements were conducted with no load on the distal output shaft, as the purpose of this testing was to establish maximal speed estimates and determine workspace asymmetries.

B. Pronation Module Evaluation

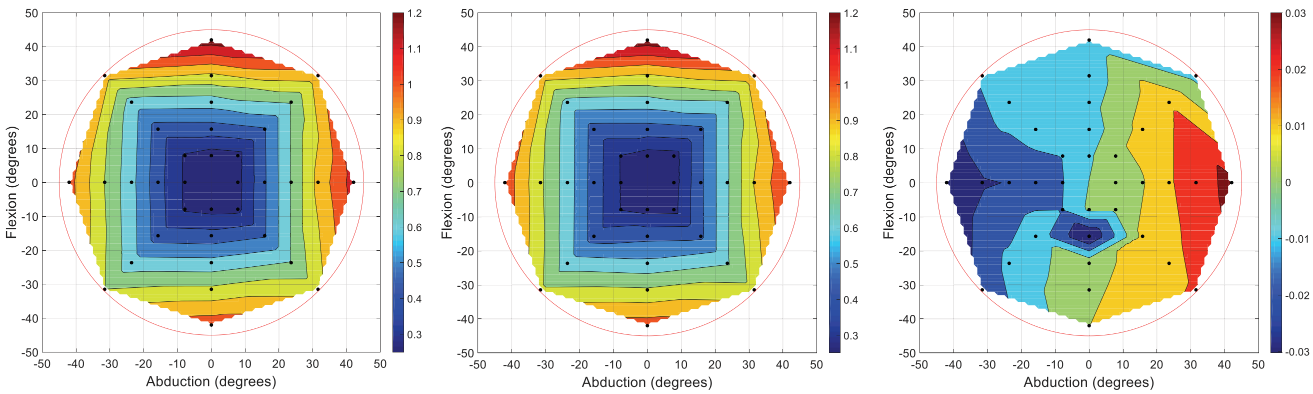

Fig. 6. Actuation times and time discrepancy. The black points are the sampled positions, and the colored contours are the interpolated data (Left) Time it takes to actuate from the neutral position (0,0) to the point in the workspace. (Center) Time to return from point on the workspace to the center. (Right) Difference between the time to actuate to point versus the reverse path.

As the load on the pronation module is generally unaffected by the flexion and abduction position, the speed of pronation was measured at 10 random points throughout the circumduction workspace. The time it took to complete 10 rotations in either direction was measured and averaged. The pronation actuator was controlled in the same way as the linear actuators (microcontroller, H-Bridge, bang-bang control).

IV. Results

A. Parallel Mechanism

To create estimates of speed over the rest of the unsampled workspace, uniformly spaced points within the workspace were had their relative actuation times interpolated. The interpolated results of actuation time from the center to a workspace point, the reverse path, and the difference between the two may be seen in Fig. 6. At positions that were actually sampled, the contours exactly match the actuation time. Performance of the individual flexion and abduction modules can be determined by looking at the points in a purely vertical line for the flexion mechanism and the points that lie on a horizontal line for the abduction mechanism.

Fig. 6 shows that the wrist can aptly actuate to any workspace extreme from the center in 1.2 seconds. This means the wrist can actuate from one extreme to another in 2.4 seconds under no load, about 20% lower than the actuators' no-load speed would predict. Moreover, the differences between moving towards or away from the neutral position are very small, on the order of hundredths of a second, though the wrist does move slightly faster when abducting (retracting the abduction actuator).

It appears that moving diagonally with both motors active in may result in faster actuation than if only a single motor is moving, hence the square pattern in the left plots of Fig. 6. This is likely because the motors are neither torque nor current limited in this load regime, but namely speed limited. As a result, the motion and loading of one actuator is barely affected by the other. For example, moving from a 0° to 30º of flexion while he abduction actuator is inactive, or when it is doing the same actuation pattern does not significantly change the load on the flexion actuator, thus it does not change the speed of either motor when moving alone or together.

The torque differences between extremes of the workspace do not seem to be significant under this loading. The maximally flexed position takes approximately 0.1 seconds less to reach (or return from) than the maximally extended position. This aligns with the torque difference expected from the kinematic analysis. The difference is approximately the same between abducted and adducted positions, with the adducted position the slower of the two. However, these torque differences may manifest as larger time differences when under more significant loading.

While the kinematic design and load capacity of this prototype look promising, the linear actuators utilized in the design result in significant overall length of the entire mechanism. In successive iterations, these motors will be replaced by more compact and lighter actuators.

B. Pronation Module

The performance of the pronation module was largely unaffected by changing the circumduction position of the wrist. On average, the wrist completed a single rotation in 3.42 seconds irrespective of flexion angle, abduction angle, or direction. This corresponds to an average rotational speed of 17.54 rpm, an 8% reduction from the expected no load speed.

This pronation speed is comparable to the OttoBock wrist rotator speed (80°/s), and approximately a half as fast as the wrist presented by Kyberd et. al in [18] (175º/s). It theoretically has significantly more torque than the Kyberd wrist, though this wrist weights about 3 times as much.

Aside from the friction in the gearbox, the pronation module has very little friction and can be easily driven by hand if the motor is not coupled. When coupled, the pronation drive is nearly nonbackdrivable, and cannot be turned without the pulleys slipping on the shafts when the motor terminals are shorted (acting like an electronic brake).

V. Conclusion

In this work we present the initial design of a 3DoF standalone prosthetic wrist device. All of the actuators in the wrist may be positioned quite freely, as long as they remain parallel to their intended lines of action (chosen in kinematic optimization). This allows for different residual limbs to be accommodated while maintaining the same kinematic architecture, control, and performance.

We conduct initial benchtop testing to evaluate the speed of the design and potential issues. Evaluating the torque capacity of the wrist and further optimizing the mechanical design to reduce weight likely must be conducted before subject testing using the device. To make this device suitable for individuals with transradial amputation, the overall length must be significantly reduced, which can be accomplished by placing actuators in parallel or embedded into the socket. Weight reduction may be accomplished through mechanical design optimization and through more complex fabrication methods employed in the construction of this prototype.

Furthermore, a method to control the wrist must be determined prior to subject testing, whether by mapping EMG signals, using pattern recognition, IMUs as in [19], or by using a combination of input devices.

REFERENCES

[1] C. M. Gosselin, E. St. Pierre, and M. Gagné, "On the Development of the Agile Eye," *IEEE Robotics and Automation Magazine*, vol. 3, no. 4, pp. 29–37, Dec-1996.

[2] B. M. Schena, "Robotic Arm with Five-Bar Spherical Linkage," US 2012/0184968 A1, 2012.

[3] P. Vischer, "Argos: A Novel 3-DoF Parallel Wrist Mechanism," *Int. J. Rob. Res.*, vol. 19, pp. 5–11, 2000.

[4] S. L. Carey, M. Jason Highsmith, M. E. Maitland, and R. V. Dubey, "Compensatory movements of transradial prosthesis users during common tasks," *Clin. Biomech.*, vol. 23, no. 9, pp. 1128–1135, 2008.

[5] B. D. Adams, N. M. Grosland, D. M. Murphy, and M. McCullough, "Impact of impaired wrist motion on hand and upper-extremity performance," *J. Hand Surg. Am.*, vol. 28, no. 6, pp. 898–903, Nov. 2003.

[6] N. M. Bajaj, A. J. Spiers, and A. M. Dollar, "State of the art in prosthetic wrists: Commercial and research devices," in *IEEE International Conference on Rehabilitation Robotics*, 2015, pp. 331–338.

[7] F. Montagnani, M. Controzzi, C. Cipriani, and S. Member, "Preliminary Design and Development of a two Degrees of Freedom passive compliant prosthetic wrist with switchable stiffness," in *ROBIO*, 2013, no. December, pp. 310–315.

[8] F. Montagnani, G. Smit, M. Controzzi, C. Cipriani, and D. H. Plettenburg, "A passive wrist with switchable stiffness for a body-powered hydraulically actuated hand prosthesis," *IEEE Int. Conf. Rehabil. Robot.*, pp. 1197–1202, 2017.

[9] F. Montagnani, M. Controzzi, and C. Cipriani, "Is it Finger or Wrist Dexterity That is Missing in Current Hand Prostheses?," *IEEE Trans. Neural Syst. Rehabil. Eng.*, vol. 21, no. c, pp. 1–10, 2015.

[10] N. M. Bajaj and A. M. Dollar, "Kinematic Optimization of a Novel Partially Decoupled Three Degree of Freedom Hybrid Wrist Mechanism," in *IEEE International Conference on Robotics and Automation, 2018. Proceedings.*

[11] A. Tilly, *The Measure of Man and Woman: Human Factors in Design*. John Wiley & Sons, Inc, 1993.

[12] W. N. Timm, S. W. O'Driscoll, M. E. Johnson, and K. N. An, "Functional Comparison of Pronation and Supination Strengths," *J. Hand Ther.*, vol. 6, no. 3, pp. 190–193, 1993.

[13] G. Zhang, J. Du, and S. To, "Study of the workspace of a class of universal joints," *Mech. Mach. Theory*, vol. 73, pp. 244–258, 2014.

[14] "Otto Bock." [Online]. Available: http://www.ottobock.com/.

[15] R. Bellman, I. Glicksberg, and O. Gross, "ON THE 'BANG-BANG' CONTROL PROBLEM," *Q. Appl. Math.*, vol. 14, no. 1, pp. 11–18, 1956.

[16] P. A. Anderson, C. E. Chanoski, D. L. Devan, B. L. McMahon, and E. P. Whelan, "Normative study of grip and wrist flexion strength employing a BTE Work Simulator," *J. Hand Surg. Am.*, vol. 15, no. 3, pp. 420–425, 1990.

[17] L.-T. Schreiber and C. Gosselin, "Passively Driven Redundant Spherical Joint With Very Large Range of Motion," *J. Mech. Robot.*, vol. 9, no. 3, p. 31014, 2017.

[18] P. J. Kyberd *et al.*, "Two-degree-of-freedom powered prosthetic wrist," *J. Rehabil. Res. Dev.*, vol. 48, no. 6, p. 609, 2011.

[19] D. A. Bennett and M. Goldfarb, "IMU-Based Wrist Rotation Control of a Transradial Myoelectric Prosthesis," *IEEE Trans. Neural Syst. Rehabil. Eng.*, vol. 26, no. 2, pp. 419–427, 2018.